Enhanced heat transfer in an onboard charging module for electric vehicles using a hybrid cooling system

Ricardo B. Juarez-Valencia[a], J.J Orta-Diaz[b], Carlo S. Sanchez-Tovar[c] J. Luis Luviano-Ortiz[d], Abel Hernandez-Guerrero[e,*]

[a]Universidad de Guanajuato, Mexico, rb.juarezvalencia@ugto.mx
[b]Universidad de Guanajuato, Mexico, jdj.ortadiaz@ugto.mx
[c]Universidad de Guanajuato, Mexico, cs.sancheztovar@ugto.mx
[d]Universidad de Guanajuato, Mexico, luis.luviano@ugto.mx
[e,]Universidad de Guanajuato, Mexico, abel@ugto.mx, corresponding author*

Abstract:

This work covers the analysis and simulation of the cooling of an on-board charging module used in electric vehicles. Advances in charging modules for electric vehicles have significantly reduced battery charging times. Due to their compact size and high-power density, effective heat dissipation is essential to maintain a suitable operating temperature. This article proposes a hybrid cooling system for a 20-kW integrated charging module. The proposed system uses water as a cooling fluid and considers operational reliability criteria. The flow rate, pressure drop, and coolant temperature profiles were obtained through numerical simulation. The results show that the proposed cooling system can keep the module's critical components below the operating temperature limit, achieving adequate and uniform cooling of the entire assembly of elements. Thus, the proposed cooling system is a viable alternative for high-power applications in compact charging modules and paves the way for modules with greater power capacity.

Keywords: Cold plate; Hybrid Cooling System; Heat Dissipation; Onboard Charger (OBC); Thermal Management.

1. Introduction

The global increase in the number of vehicles significantly impacts greenhouse gas emissions, since most vehicles rely on fossil fuels [1]. This renders them unsuitable as a long-term solution, driving the search for less harmful alternatives [2]. Electric vehicles (EVs) have the potential to significantly reduce these emissions. However, the transition to electric transportation requires reliable energy storage and supply, with fast charging and slow discharging. Although lithium-ion battery technology has advanced considerably, using various thermal management strategies to extend battery service life [3], the focus is currently on charging modules, as they supply power to Li-ion batteries. Since charging times are fairly long under optimal conditions [4], efforts are being made to reduce this time without causing overheating in the charging module components.

Advances in charging module technology for electric vehicles are limited by battery charging speed. This causes the components to reach high temperatures, resulting in severe damage to the charging modules, especially the metal-oxide-semiconductor field-effect transistors (MOSFETs). MOSFETs are semiconductor devices that switch or amplify signals in electronic circuits. MOSFETs operate using a small voltage at their gate terminal to create an electric field that controls the flow of a much larger current between the source and drain terminals. Emerging ultra-fast charging technology (XFC) [5] has the potential to provide an experience similar to that of gasoline-powered vehicles. While vital for efficient power management and high-speed switching, MOSFETs often exceed their operating temperature.

Maintaining the components at an optimal operating temperature requires more than one cooling method. Otherwise, their service life is reduced by more than half. Effective thermal management is

essential to ensure the reliable operation of charging modules and enable higher charging speeds and power densities. Thermal dissipation techniques implemented thus far include immersing magnetic components in epoxy resin, using forced convection systems with fans [6], heat pipes (HP), and other techniques described in [6]. Although HP [7–8] are an excellent option for thermal management [9], even when the designs are very thin, research [10] into the effect of the ratio of liquid-to-vapor flow cross-sectional areas on heat dissipation performance has shown that these designs are limited [11], as they only focus on a small number of components. Another method [12] of heat dissipation in confined spaces, where electronic components are located within load modules, is indirect air cooling using forced convection systems [13]. Research has also been conducted on the interaction between cooling architecture and PCB design [4]. Alternative methods, such as liquid cooling, are also employed to cool charging modules. Liquid cooling is a method [14] that has been used in power electronics in conjunction with co-design and co-simulation. This same method [15] has also been used for fast-charging systems.

Another approach to controlling component temperature is to improve the module's efficiency. Developments are not limited to thermal management but also involve hardware development [16]. Similarly, studies have been conducted on power flow, short-circuit protection, and hardware protection [17]. Charging module efficiency is an area that is constantly being evaluated [18], and Rafi and Bauman are among the researchers working to reduce parasitic losses. They are also using WBG semiconductors to create a CLLC resonant converter [19] and optimizing magnetic component design [20] to reduce parasitic capacitance and increase charging module efficiency. There have been advances in energy transfer development with the implementation of DC chargers, which reduce energy losses and transistor temperature. Despite these advances, challenges remain [21], such as concerns regarding battery life and the relatively low energy density of 200–300 Wh/kg in lithium-ion batteries (compared with 13,000 Wh/kg for gasoline) and the lack of public charging infrastructure. These issues remain significant barriers to the widespread adoption of EVs.

This work explores a hybrid water-and-air based heat dissipation system, implementing a cooling method similar to that of Zeng [22]. The goal is to ensure that all components within the module reach an optimal operating temperature, even during full load charging. The analysis focuses on a 20-kW commercial-grade DC model, which experiences losses around 5% at full load, corresponding to approximately 1 kW of heat dissipation. This heat is primarily generated by components such as MOSFETs and chips. Straight rectangular fins are implemented on components that generate the most heat, and a cold plate based on a six-step model covers most of the remaining components.

2. Methodology

2.1. Geometric model

The geometric model implemented was based on a 20-kW commercial charging module (Figure 1). The dimensions of the module are 470 mm × 206 mm × 83 mm, as shown in Figure. 1 a). The 2 mm-thick casing is equipped with two fans that provide a total airflow of 134.292 CFM, as shown in Figure 1 b). The maximum efficiency of 20 kW load modules typically ranges from 94% and 96%. For this specific model, the maximum efficiency was 96% at full load. The CAD of this model is shown in Figure 2.

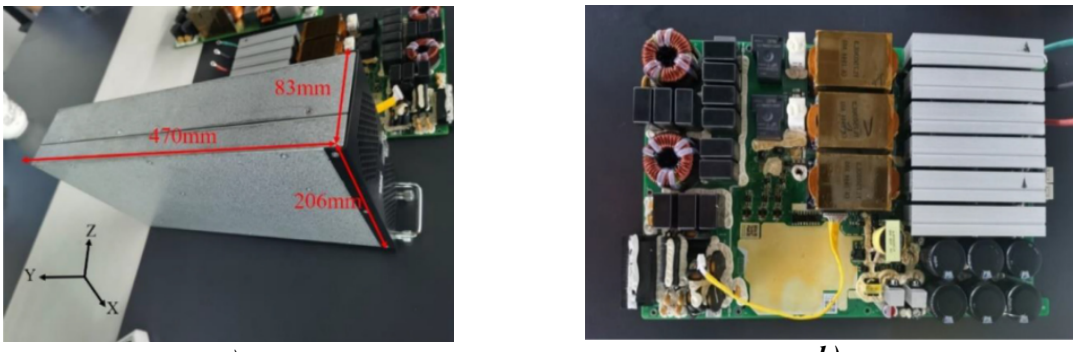

a) ***b)***

Figure 1. *Commercial 20-kW module (images courtesy of [11]).* ***a)*** *module dimensions;* ***b)*** *main components.*

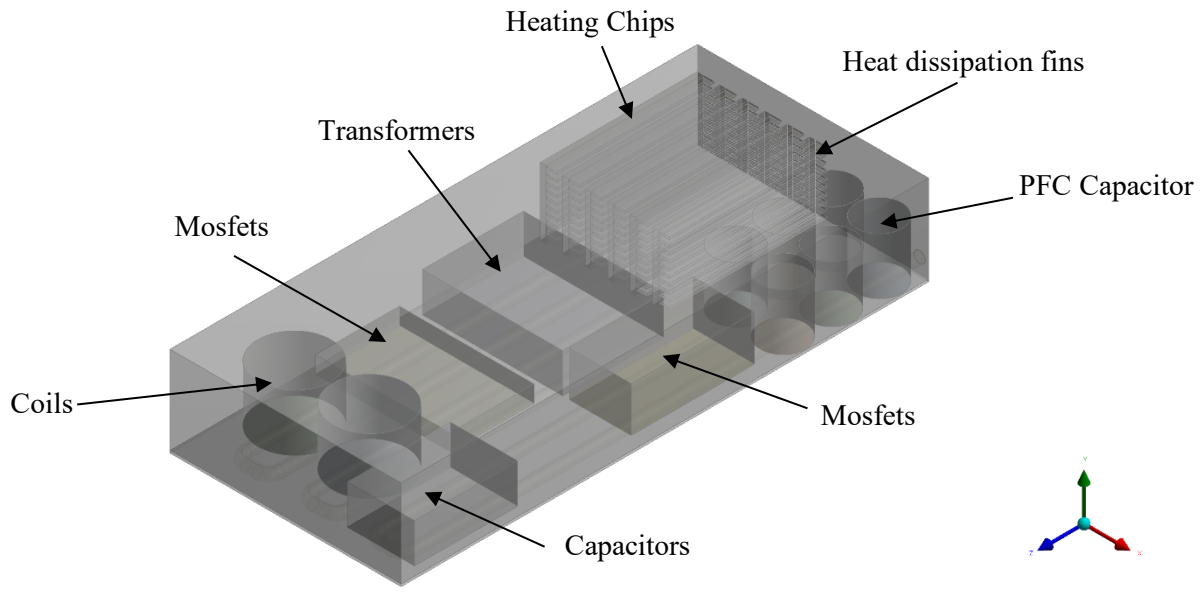

Figure 2. *CAD model of a 20-kW commercial module.*

This analysis involved thermal modeling of each component of the load module under full-load operations, i.e., at a maximum efficiency of 96%. Table 1 presents the thermal properties and heat generation of each component, which were taken from [24].

Table 1: Properties of the charging module components.

Components	Material	ρ (kg/m^3)	k (W/m · K)	c_p (J/kg · K)	q'''(kW/m^3)
Chip	Silicon	2330	148	712	2380.95
Capacitors (PFC)	Aluminum	2719	202.4	871	318.31
Coils		4900	4	800	301.36
Mosfet	Silicon	2329	150	700	413.22
Transformer		1250	5	1300	533.33
Fins	Aluminum	2719	202.4	871	
PCB	FR4	1750	16.5	1000	
Housing	Aluminum	2719	202.4	871	
Cooling fluid	Air	1.176	0.0261	1.0063	
Cooling fluid	Water	996.5	0.6103	4181	

2.2. Numerical model

A numerical analysis of the module was performed using ANSYS Workbench 2019 R3, considering the heat generation of each component and applying standard temperature and pressure boundary conditions. Inspired by the simplified model proposed by [11], a geometric simplification of the commercial model was implemented without compromising the simulation results. The numerical method involves solving the momentum, continuity, and energy equations, along with suitable boundary conditions.

Momentum conservation equation:

Assuming steady-state, incompressible, Newtonian flow with constant properties and no body forces, the momentum equation was simplified, resulting in the classical form of the Navier–Stokes equations:

$$\rho(\boldsymbol{V} \cdot \nabla)\boldsymbol{V} = -\nabla p + \mu\nabla^2\boldsymbol{V} \tag{1}$$

Energy conservation equation:

The energy equation was solved assuming steady-state conditions, constant thermophysical properties, and neglecting viscous dissipation, resulting in a convection-diffusion formulation:

$$\rho C_p(\boldsymbol{V} \cdot \nabla T) = k\nabla^2\mathrm{T} \tag{2}$$

Continuity equation:

The continuity equation was simplified assuming steady-state, incompressible flow:

$$\nabla \cdot \mathbf{w} = 0 \tag{3}$$

Reynolds number:
For the Reynolds number calculations, the properties of water were taken at 300 K, resulting in a Re value of 10,500:

$$Re = \frac{\rho VD}{\mu} \tag{4}$$

Nusselt number:
For fully developed turbulent flow conditions and a Prandtl number of 5.83, the Dittus–Boelter Equation was used, obtaining a Nu value of 77:

$$Nu_D = 0.023 Re_D^{4/5} Pr^{0.4} \tag{5}$$

Friction factor:
For fully developed turbulent flow conditions and smooth walls, the following equation was used to obtain the friction factor, obtaining an *f* value of 0.031:

$$f = (0.790 \ln Re_D - 1.64)^{-2} \tag{6}$$

Convection coefficient:
For a diameter of 10 mm and the thermal conductivity of water at 300 K, Equation (7) was used, obtaining a convection coefficient value of 4,700 W / (m² K):

$$h = \frac{N_u k}{D} \tag{7}$$

2.3. Cold plate selection

To ensure adequate cooling of the module's internal components, a pipe geometry was selected to accommodate as many components as possible within the available space. Due to the limited internal space, a model based on the commercial design of Cold Plate 416201U00000G (see Figure 3) and the inlets and outlets of water and air within the model were identified (see Figure 4). The dimensions of the cold plate were adapted for the load module studied in this article, with a tube diameter of 10 mm and a total flow path length of 2750 mm.

Figure 3. *Commercial cold plate.*

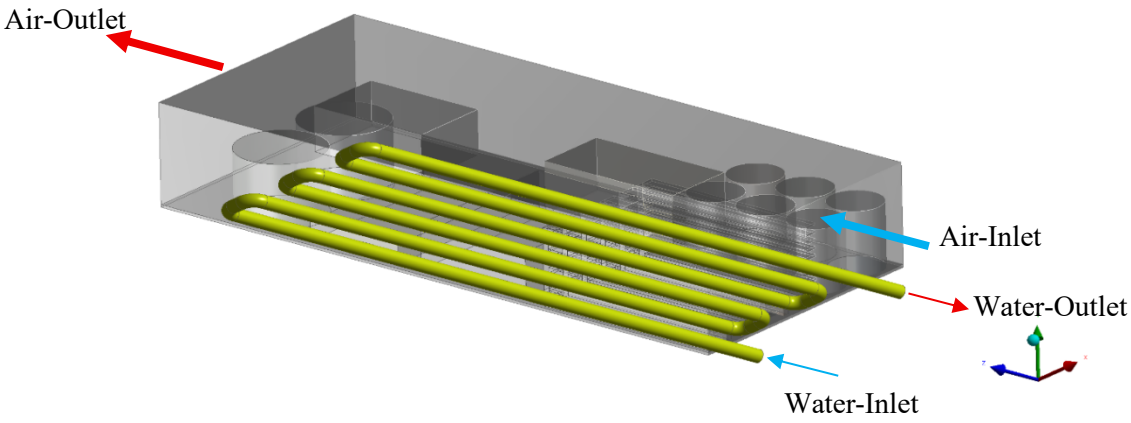

Figure 4. *Cold plate implemented in the CAD model.*

2.4. Choosing the fins

The cooling system fins are straight and rectangular because this geometry provides the most effective heat dissipation among the configurations analyzed. The fins are 2 mm long, 140 mm wide, and 10 mm high. Due to weight constraints and the high heat generation of the chips, aluminum was applied only to these components, enabling more effective use of the module's air intake.

2.5. Boundary conditions

For the simulation, a constant water inlet velocity of 0.9 was imposed, resulting in a Reynolds number of 10,500, with the outlet set to atmospheric pressure. Air was assumed to be at 27 °C, with an inlet velocity of 3 m/s, corresponding to a Reynolds number of 22,328, and an outlet at atmospheric pressure. The thermophysical properties of both fluids were evaluated at 27 °C. The thermophysical properties and volumetric heat generation of the components are listed in Table 1 under full-load conditions. Both water and air were considered incompressible fluids (as the Mach number for air is 0.0086 < 0.3, indicating negligible compressibility effects and minimal density variation). Based on these conditions, the SST k-omega turbulence model was selected because it effectively captures turbulent behavior and accurately resolves velocity gradients.

2.6. Validation

Three simulation cases are presented to validate the properties of the electrical components and the physical conditions to which the charging modules are subjected. Each case corresponds to a different study, and the corresponding source is referenced in each subsection.

Case I

To ensure that the simulation accurately represents real operating conditions, commercial data on the electronic components comprising the fast-charging module were used. Silicon carbide MOSFETs are of particular importance due to the significant thermal loads they impose on the PCB. These devices are widely used for high-voltage operation in compact systems and to enhance switching frequency; however, these operating conditions lead to increased temperatures in the electronic components.

In this context, 16 Wolfspeed C3M0065090J MOSFETs, each dissipating 5W, were simulated, with a spacing of 30 mm between them (Figure. 5). The devices were arranged on the same cold plate geometry used as a reference for the main charging module.

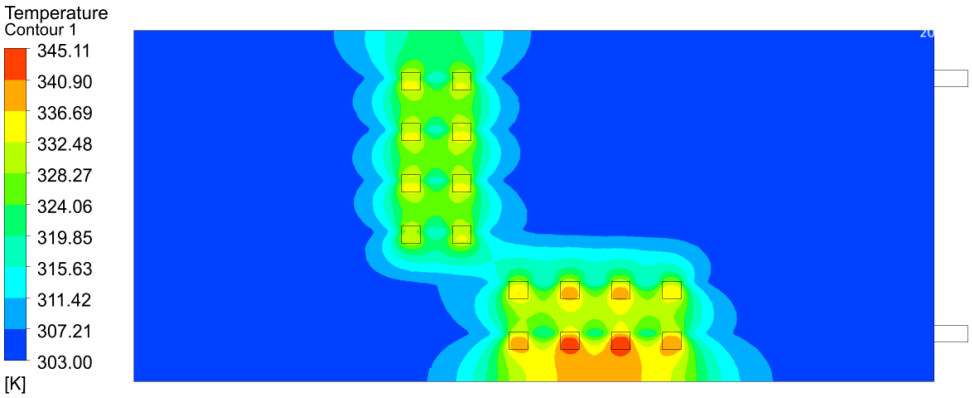

Figure 5. *Temperature of the MOSFETs operating at 5W.*

Case II

Table 2 presents the experimental and numerical results reported by [11], along with the corresponding deviation values. Figure 6 shows the numerical simulation results obtained in this study, with an error of less than 5%. These results indicate a temperature difference of approximately 2 °C compared to the experimental data in Table 2, thereby validating the model's ability to reproduce the behavior of the physical system.

Table 2: *Experimental temperature report* shown in [3].

	Number of measuring point	Experiment (°C) Steady	Simulation result (°C) Max	Min	Deviation
PFC	116	49.7	45.97	45.35	8.771%
Capacitor			46.17	45.42	

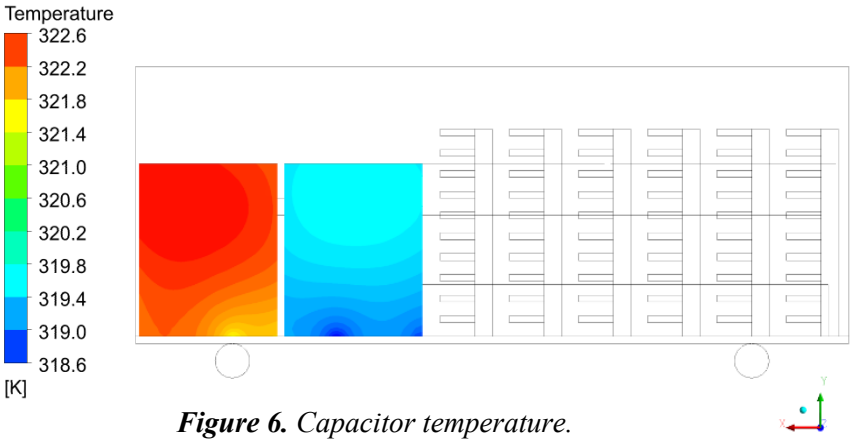

Figure 6. *Capacitor temperature.*

Case III

A numerical simulation was carried out for Case III, as reported by [6]. This simulation represents the thermal performance of the cooling system with a cold plate applied to the MOSFETs.

The results showed a margin of error of 2% compared to the reference data. This corresponds to an approximate temperature difference of 8 °C in the pipe mounting region, while the temperature variation across the MOSFETs remains close to 1 °C. However, an exception was identified in the upper left corner of the domain, where the thermal variation reaches approximately 8 °C, as illustrated in Figure 7.

These results support the validity of the methodology employed, particularly in the characterization of the physical properties used to simulate the cooling process of both the MOSFETs and the cold plate.

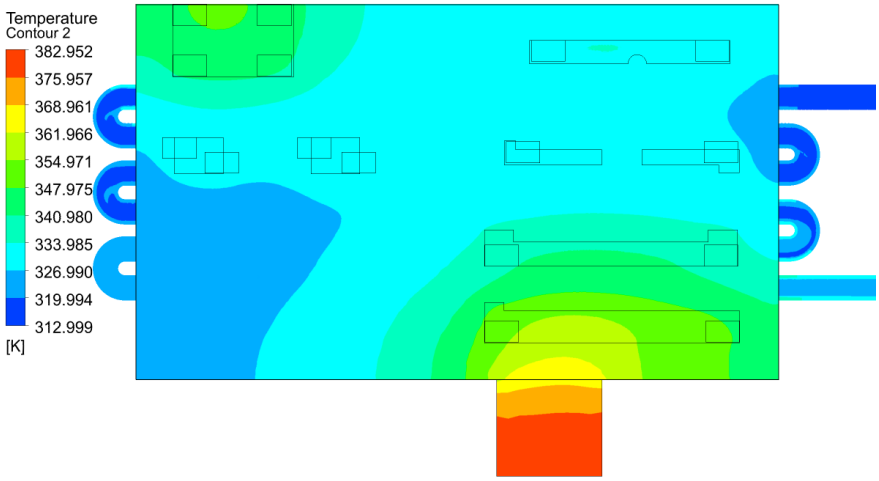

Figure. *7 Temperature of the geometry replicated in [3].*

2.7. Mesh independence

The following results present the findings of the mesh analysis. The temperature at various points along capacitors, using meshes with significantly different numbers of elements, was taken as a reference, as shown in Figure 8. To ensure mesh independence, element sizes of 2.5 mm, 2 mm, and 1.5 mm were considered. The 2.5 mm mesh, consisting of 3,418,620 elements, was selected, because it provides an appropriate balance between accuracy and computational cost, with temperature differences below 4% among the tested meshes.

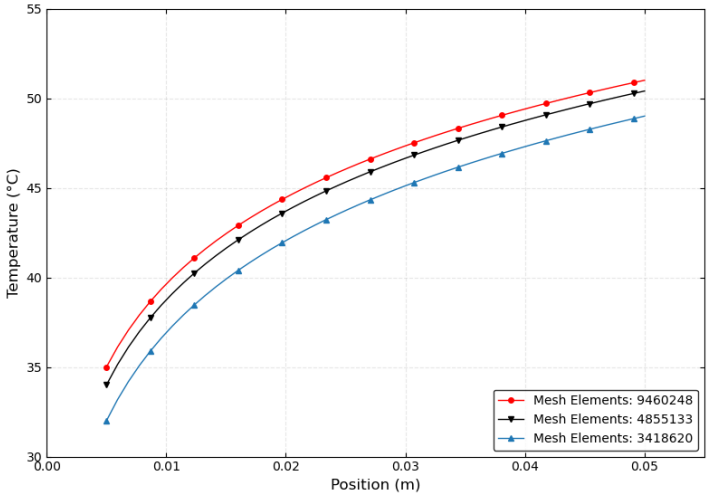

Figure 8. *Mesh Independence.*

3. Results and discussion

3.1. Cold plate

Different configurations and fluid inlet velocities were evaluated for the implemented Cold Plate Model to determine the most effective arrangement for heat dissipation from the electronic components. Certain combinations of diameter and inlet velocity were found to significantly improve thermal performance without causing excessive pressure drop. Commercial Cold Plate models typically use pipe diameters ranging from 9 to 10 mm. Unlike these, the simulation model presented in this study considers a wider range of diameters (6-14 mm) and inlet velocities (0.5-1.3 m/s) to analyze their effect on thermal performance. Within this range, a diameter of 10 mm combined with an inlet velocity of 0.9 m/s yielded one of the best results, achieving 626 W of heat dissipation with a pressure drop of 5,220 Pa. Under these conditions, most components operated within an acceptable temperature range.

The subfigures in Figure 9 show a top-down view of the temperature profiles of the components when using the cold plate. Figure 9 presents temperature profiles at different module heights to illustrate the influence of the cold plate on the electronic components.

At the PCB level (Figure 9 a), the influence of the cold plate on both the component bases and the PCB is evident, maintaining most components within a suitable temperature range, with localized exceptions where its effect is limited. At a height of 5 mm (Figure 9b)), a similar thermal behavior is observed, indicating efficient heat dissipation in this region. At 10 mm (Figure 9c)), an increase in temperature appears in the transistors, with differences of approximately 6 °C compared to other zones. At greater heights (15 mm and 20 mm; Figures 9 d) and 9 e), respectively), the influence of the cold plate decreases progressively, leading to higher temperatures in components such as transistors and coils.

Nevertheless, temperatures remain within safe operating limits. In particular, the transistors reach approximately 100 °C at 20 mm above the PCB, which is below their estimated critical temperature of 150 °C, ensuring the operational integrity of the system.

Conclusion

This study proposes and evaluates two thermal management strategies to maintain the temperature of electronic components within safe limits while avoiding the incorporation of additional elements that could compromise overall system performance. Numerical models were developed to accurately reproduce the physical behavior of charging modules, thereby enabling validation of the proposed solutions, with deviation below 5% when compared to experimental and literature data, confirming the reliability of the simulation approach.

The first strategy involved implementing 2-mm-thick, straight rectangular fins on one side of each chip. This configuration reduced the temperature by 3 to 4 °C. However, increasing the fin thickness resulted in only marginal thermal improvements (1–2 °C), indicating that a thickness of 2 mm provides an effective thermal solution, while also highlighting the importance of geometric optimization under space and weight constrains in compact power electronic systems.

The second strategy relied on the use of a cold plate, whose performance was evaluated through parametric simulations considering variations in pipe diameter (6–14 mm) and fluid inlet velocity (0.5–1.2 m/s). The results showed that the combination of a 10 mm diameter and an inlet velocity of 0.9 m/s provides an effective balance between heat dissipation and pressure drop, allowing most electronic components to be maintained at approximately 80 °C within the regions directly influenced by the cooling system, while achieving a heat dissipation capacity of up to 626 W and maintaining acceptable hydraulic performance (pressure drop of 5,220 Pa).

Additionally, the study focused on ensuring efficient thermal management within the spatial constraints of charging modules, demonstrating that the proposed hybrid cooling approach can handle thermal loads on the order of 1 kW under full-load operating conditions without exceeding critical temperature limits.

As a direction for future research, the implementation of a third complementary method is proposed, such as the use of 50% water–glycol mixtures as a coolant, along with other possible modifications. This approach aims to further enhance heat dissipation capacity and enable the development of higher power density modules.

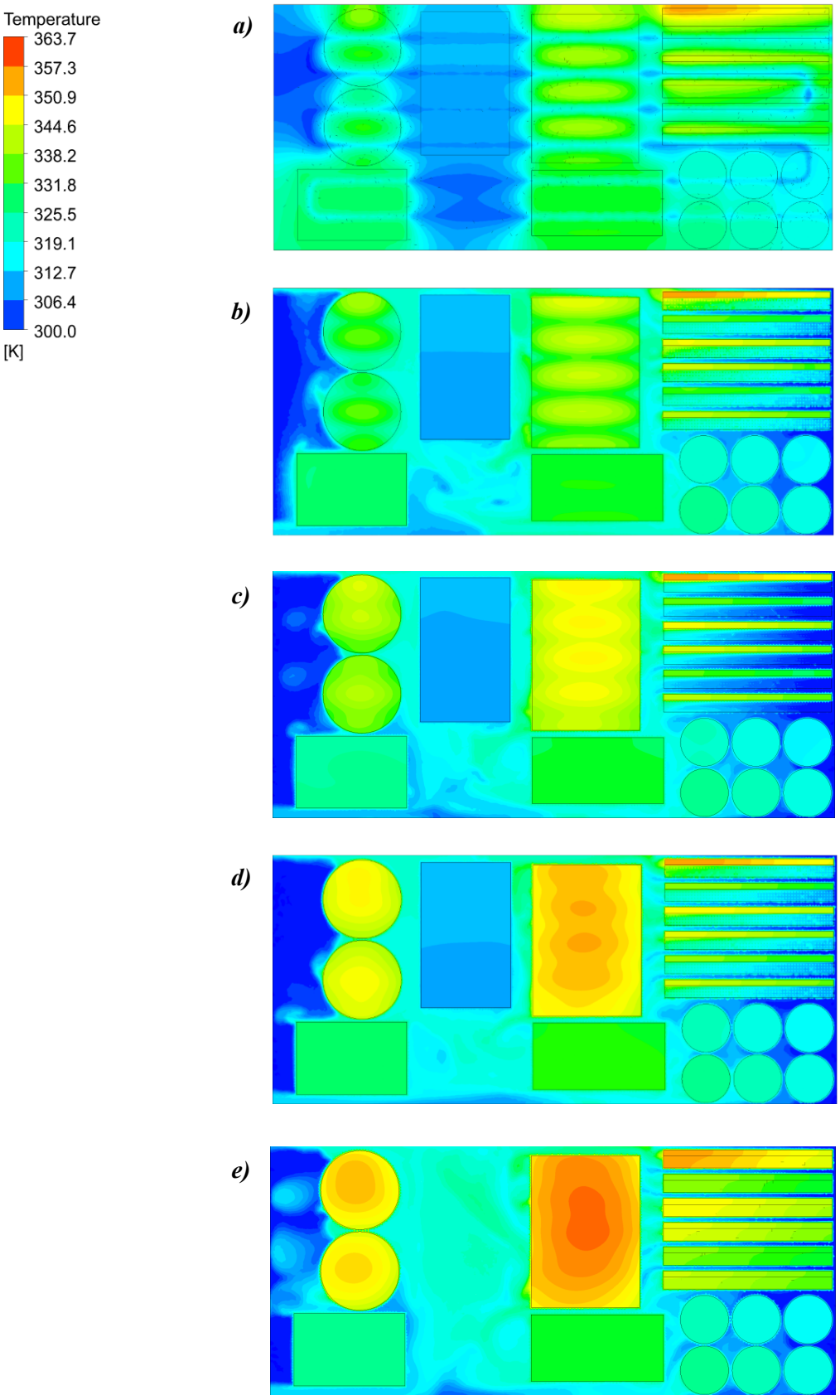

Figure 9. Temperature profiles at different heights above the PCB: a) 0 mm; b) 5 mm; c) 10 mm; d) 15 mm; e) 20 mm.

References

[1] Mohamet, S. A., Jung, J. W., 2021, A Comprehensive State-of-the-Art Review of Wired/Wireless Charging Technologies for Battery Electric Vehicles: Classification/Common Topologies/Future Research Issues, IEEE access, volume 9, pp. 19572-19585, doi: 10.1109/ACCESS.2021.3055027.

[2] Lamb, W.; Wiedmann, T.; Pongratz, J.; Andrew, R.; Crippa, M.; Olivier, J., et al. (2021). A review of trends and drivers of greenhouse gas emissions by sector from 1990 to 2018. Environmental Research Letters, 16(7), 073005. Report #: ARTN 073005. OSTI ID: 1973647. http://dx.doi.org/10.1088/1748-9326/abee4e.

[3] Yuksel, T., Litster, S., Viswanathan, V., Michalek, J., 2017, Plug-in hybrid electric vehicle LiFePO4 battery life implications of thermal management, driving conditions, and regional climate, Journal of Power Sources, Volume 338, pp. 49-64, ISSN 0378-7753, https://doi.org/10.1016/j.jpowsour.2016.10.104.

[4] Tayyara, O., Gupta, K., Da Silva, C., Nasr, M., Assadi, A., Trescases, O., Amon, CH., 2019, "Effects of Cooling Architecture and PCB Layout Co-Design on the Concurrent Thermal and Electrical Performance of an On-Board Electric Vehicle Charger." Proceedings of the ASME 2019 International Technical Conference and Exhibition on Packaging and Integration of Electronic and Photonic Microsystems. ASME 2019 International Technical Conference and Exhibition on Packaging and Integration of Electronic and Photonic Microsystems. Anaheim, California, USA. October 7–9, 2019. V001T06A012. ASME. https://doi.org/10.1115/IPACK2019-6434.

[5] Tu, H., Feng, H., Srdic, S., Lukic, S., 2019, "Extreme Fast Charging of Electric Vehicles: A Technology Overview," in IEEE Transactions on Transportation Electrification, vol. 5, no. 4, pp. 861-878, doi: 10.1109/TTE.2019.2958709.

[6] Gupta, K., Da Silva, C., Nasr, M., Assadi, A., Matsumoto, H., Trescases, O., Amon, C. H., 2018, Thermal Management Strategies for a High-Frequency, Bi-Directional, On-Board Electric Vehicle Charger. 17th IEEE Intersociety Conference on Thermal and Thermomechanical Phenomena in Electronic Systems (ITherm) pp. 935-943. doi:10.1109/ITHERM.2018.8419580.

[7] Clepcea, B. I., 2025, CFD Simulation of a Novel Planar Heat Pipe for Battery Cooling and Heating in Electric Vehicles, Lappeenranta–Lahti University of Technology LUT LUT School of Energy Systems Degree Programme in Energy Technology In co-operation with partner university: HEBEI University of Technology.

[8] Li, Y., He, Y., Bai, X., Tao, H., 2026, Thermal analysis of an enclosed charging module with a heat pipe-based independent air duct cooling system. International Journal of Thermal Sciences, Volume 219, 110198, ISSN 1290-0729, https://doi.org/10.1016/j.ijthermalsci.2025.110198.

[9] Yan, W., Yang, X., Liu, T., Wang S., 2023, Numerical Simulation of Heat Transfer Performance for Ultra-Thin Flat Heat Pipe. J. Therm. Sci. 32, pp. 643–649. https://doi.org/10.1007/s11630-023-1768-0.

[10] Zhou, W., Li, Y., Chen, Z., Deng, L., Gan, Y., 2019, Effect of the passage area ratio of liquid to vapor on an ultra-thin flattened heat pipe, Applied Thermal Engineering, Volume 162, 114215, ISSN 1359-4311, https://doi.org/10.1016/j.applthermaleng.2019.114215.

[11] Ming, T., Liao, X., Shi, T., Yin, k., Wang, Z., Ahmadi, M., Wu, Y., 2023, The thermal analysis of the heat dissipation system of the charging module integrated with ultra-thin heat pipes. Energy and Built Environment, Volume 4, Issue 5, pp. 506-515, ISSN 2666-1233, https://doi.org/10.1016/j.enbenv.2022.03.007.

[12] Kim, J., Choe, G., Jung, H., Lee, B., Cho, Y., Han, K., 2010, Design and Implementation of a High-Efficiency OnBoard Battery Charger for Electric Vehicles with Frequency Control Strategy. Vehicle Power and Propulsion Conference (VPPC) IEEE, doi: 10.1109/VPPC.2010.5729042.

[13] Biela, J., Kolar, j. W., 2007, "Cooling Concepts for High Power Density Magnetic Devices," Power Conversion Conference - Nagoya, Nagoya, Japan, 2007, pp. 1-8, doi: 10.1109/PCCON.2007.372915.

[14] Assadi, S. A., Tayyara, O., Palumbo, J., Chen, A., Zaman, M. S., Da Silva, C., Chandra, S., Amon, C. H., Trescases, O., 2023, "Electro-Thermal Co-design of a High-Density Power-Stage for a Reconfigurable-Battery-Assisted Electric-Vehicle Fast-Charger using Multi-Physics Co-simulation and Topology Optimization," IEEE Applied Power Electronics

Conference and Exposition (APEC), Orlando, FL, USA, pp. 1808-1815, doi: 10.1109/APEC43580.2023.10131627.

[15] Palumbo, J., Tayyara, O., Assadi, S. A., Da Silva, C., Trescases, O., Amon, C. H., Chandra, S., 2024, Thermal Management of Non-Uniform Heat Fluxes in an Electric-Vehicle Fast-Charger: Experimental and Numerical Analysis. IEEE Transactions on Components, Packaging and Manufacturing Technology. pp. 573-584, doi: 10.1109/TCPMT.2024.3376993.

[16] Tobón-Ramírez, D. A., & Restrepo-Laverde, J. V. (2018). Desarrollo de estación de carga de vehículos eléctricos. Lámpsakos (revista Descontinuada), 1(19), pp. 22–29. https://doi.org/10.21501/21454086.2532.

[17] Etezadi, A. M., Choma, k., Estefani, J., 2010, Rapid-Charge Electric-Vehicle Stations, IEEE transactions on power delivery, vol. 25, no. 3, pp. 1883-1887, doi: 10.1109/TPWRD.2010.2047874.

[18] Rafi, A., Bauman, J., (2020). A Comprehensive Review of DC Fast-Charging Stations With Energy Storage: Architectures, Power Converters, and Analysis. IEEE Transactions on Transportation Electrification. PP. 99-1114, doi: 10.1109/TTE.2020.3015743.

[19] Zhang, Z., Liu, C., Wang, M., Si, Y., Liu, Y., Lei, Q., 2020, "High-Efficiency High-Power-Density CLLC Resonant Converter With Low-Stray-Capacitance and Well-Heat-Dissipated Planar Transformer for EV On-Board Charger," in IEEE Transactions on Power Electronics, vol. 35, no. 10, pp. 10831-10851, doi: 10.1109/TPEL.2020.2980313.

[20] Wouters, H., Martinez, W., 2024, "Bidirectional Onboard Chargers for Electric Vehicles: State-of-the-Art and Future Trends". IEEE Transactions on Power Electronics, vol. 39, no. 1, pp. 693-716, Jan. 2024, doi: 10.1109/TPEL.2023.3319996.

[21] Oladigbolu, J., Mujeeb, A., Li, L., 2024, Optimization and energy management strategies, challenges, advances, and prospects in electric vehicles and their charging infrastructures: A comprehensive review, Computers and Electrical Engineering, Volume 120, Part C, 109842, ISSN 0045-7906, https://doi.org/10.1016/j.compeleceng.2024.109842.

[22] Zeng, X., Li, J., Qiao, L., Chen, M., (2024) Experimental study on the performance of power battery module heating management under a low–temperatures charging scenario, International Journal of Heat and Mass Transfer, Volume 225, 125388, ISSN 0017-9310, https://doi.org/10.1016/j.ijheatmasstransfer.2024.125388.

[23] Ki, S., Lee, J., Ryu, S., Bang, S., Kim, K., Nam, Y., 2021, A bio-inspired, low pressure drop liquid cooling system for high-power IGBT modules for EV/HEV applications, International Journal of Thermal Sciences, Volume 161, 106708, ISSN 1290-0729, https://doi.org/10.1016/j.ijthermalsci.2020.106708.

[24] Lopez, G. S., 2020, Thermal Modelling of High-Frequency Magnetic Components for Power Electronics by Finite Element Analysis. Tesis (Doctoral), E.T.S.I. Industriales (UPM). https://doi.org/10.20868/UPM.thesis.62988.